

conductors, $\bar{\omega}/W$ may be as much as a factor of 20 larger (i. e., of order 0.04 for V_3Si and Nb_3Sn). In this type of material the *average* electron-phonon-induced width is comparable with experimental resolution. Certainly in these cases, and probably in many less favorable cases as well, the phonons most important for superconductivity should have easily measurable widths. In particular, the anomalous phonons observed in Refs. 1-3 should have widths much greater than the average

width, if they arise from strong electron-phonon coupling. Furthermore, if γ_Q can be measured, the sum rule (12) allows a determination of what proportion of the coupling λ arises from anomalous regions of the spectrum. Information of this type would greatly increase our understanding of the connection between unstable lattices and high- T_c superconductors.

I am grateful to G. Shirane and J. D. Axe for stimulating my interest in this subject.

¹G. Shirane, J. D. Axe, and R. J. Birgeneau, *Solid State Commun.* **9**, 397 (1971).

²G. Shirane and J. D. Axe, *Phys. Rev. Letters* **27**, 1803 (1971).

³H. G. Smith and W. Glaser, *Phys. Rev. Letters* **25**, 1611 (1970).

⁴D. J. Scalapino, in *Superconductivity*, edited by R. D. Parks (Marcel Dekker, New York, 1969).

⁵W. L. McMillan and J. M. Rowell, in Ref. 4.

⁶W. L. McMillan, *Phys. Rev.* **167**, 331 (1968).

⁷R. C. Dynes, *Solid State Commun.* **10**, 615 (1972).

⁸I have not succeeded in proving that the Coulomb

vertex corrections to the matrix elements in Eqs. (2) and (11) are completely identical. They are at least very similar, and the error in any case should be small and slowly varying with Q . I wish to thank P. J. Feibelman for a helpful discussion on this point.

⁹Such a pathological case would be for example, the Labbé-Friedel one-dimensional model for A15 compounds, with the Fermi level as close as ω_Q to a band edge. See, for example, J. Labbé, S. Barisić, and J. Friedel, *Phys. Rev. Letters* **19**, 1039 (1967). Even in this context, Eq. (10) remains valid for low-frequency phonons.

Magnetic Flux Penetration into Superconducting Thin Films*

Gerald E. Peabody[†]

Harvard University, Cambridge, Massachusetts 02138

and

R. Meservey

Francis Bitter National Magnet Laboratory, ‡ Massachusetts Institute of Technology, Cambridge, Massachusetts 01239

(Received 20 December 1971)

The absolute value of the penetration depth in Sn and Pb superconducting thin films was measured using a quantum-interference technique. The value of the penetration depth obtained for 1500-Å-thick films of Pb was 630 Å; the value for a 3000-Å-thick film of Sn was 770 Å, and for a 2000-Å-thick film was 730 Å. These results are probably consistent with the BCS microscopic theory within the experimental error, although a direct comparison between the theoretical and experimental values is made difficult by the uncertainty in the nonlocal correction for the film thickness. The temperature dependence of the penetration depth for Pb (measured for temperature less than 4.2 K) agrees with a previous measurement of Erbach *et al.* For Sn the temperature dependence deviates from the theoretically expected behavior near the transition temperature. Results are given to show that the critical current of a superconducting interferometer with two parallel junctions is not strictly periodic in the applied magnetic flux with a period equal to the flux quantum $hc/2e$ because of the magnetic field dependence of the critical currents of the junctions.

I. INTRODUCTION

Many years ago London and London¹ predicted the existence of the penetration depth λ , the characteristic distance that a magnetic field penetrates into a superconductor. A few years later Shoenberg² obtained a measured value of λ . Since then, there have

been many measurements of the penetration depth, but only recently has it been feasible to measure the absolute value of λ .

Summaries of early penetration-depth measurements are given by Shoenberg,³ London,⁴ and Serin⁵; more recent results are described by Jaggi and Sommerhalder,⁶ Waldram,⁷ and Meservey and

Schwartz.⁸

In principle, measurements of the susceptibility of colloidal spheres,^{2,9} thin wires,¹⁰ and thin films¹¹ could give an absolute value of the penetration depth. In practice, limitations on sensitivity and uncertainty of the geometrical structure of the very small samples required have so far kept these methods from yielding anything but approximate values of λ . Quoted figures for the absolute value have generally been obtained by measuring the temperature or frequency dependence of λ and then fitting the experimental data to the best theoretical model of the parametric dependence.

Measurements of the temperature dependence of the surface reactance were made at low frequency by Laurmann and Shoenberg¹² and at 10 MHz by Schawlow and Devlin¹³ and others. At microwave frequencies, London¹⁴ made early measurements of the surface resistance from which a value of λ could be deduced. Pippard¹⁵ initiated measurements of the high-frequency surface impedance of superconductors from which he and many others have obtained values of λ (which is the zero-frequency limit of the surface reactance). The magnetic field dependence of the surface impedance was first measured by Pippard¹⁶; for more recent work see Garfunkel.¹⁷ A review and careful analysis of surface-impedance measurements have been given by Waldram,⁷ who concludes that the best absolute value of λ to date is to be inferred from measurements of the surface impedance as a function of temperature, frequency, and impurity content combined with theory in a self-consistent manner. In all of these methods it is necessary to rely on the theoretical dependence with temperature, frequency, impurity content, or magnetic field in order to obtain an absolute value of λ . In contrast to these methods the quantum-interference technique¹⁸ measures the absolute value of λ in a direct way.

The quantum-interference technique assumes that the change in phase of the superconducting wave function around any contour within the superconductor must be $2\pi n$, where n is a non-negative integer. When two superconducting weak-link junctions are placed in parallel in a superconducting loop (Fig. 1), the total supercurrent through the paired junctions will be the sum of the currents through each junction. Since there is phase coherence across each junction, there is phase coherence around the total loop, and the fluxoid must be quantized. The critical current of the junction pair is modulated by the flux enclosed within the loop and, under the proper circumstances, is periodic in the magnetic flux with a period equal to $\varphi_0 = hc/2e$, the flux quantum. Thus a measurement of the modulation of the critical current of the two-junction loop as a function of an applied magnetic

field determines the increment of applied field necessary to add one quantum of flux to the loop. The total effective area of the loop is thereby determined, and, in particular, if the dimensions of the hole are known accurately, the area of the flux penetration into the superconductor bordering the hole is determined. The absolute value of the penetration depth is obtained directly from the area of flux penetration into the superconductor and the inner perimeter of the hole. In this paper the results of such measurements are reported for experiments with lead and tin films.

II. THEORY

A. Measurements of Flux Penetration by Fluxoid Quantization

An end view of the type of sample used to determine the penetration depth is shown schematically in Fig. 1. Two superconducting films are separated by a narrow dielectric film and are joined at the edges of the dielectric by superconducting weak links. The sample is connected by the external circuit in such a way that the weak links are in parallel. The London fluxoid-quantization condition⁴ when applied to superconducting pairs¹⁹ is

$$c\oint \Lambda \vec{j}_s \cdot d\vec{l} + \oint \vec{A} \cdot d\vec{l} = n \frac{hc}{2e} = n\varphi_0, \quad (1)$$

where the contour of integration is to be within the superconducting volume. The second integral can be written

$$\oint \vec{A} \cdot d\vec{l} = \varphi = \varphi_e + Li_c, \quad (2)$$

where

$$\varphi_e = BS + \varphi_{sc}; \quad (3)$$

φ is the total flux enclosed by the loop, φ_e is the flux within the loop from the externally applied field, L is the inductance of the loop, i_c is the net

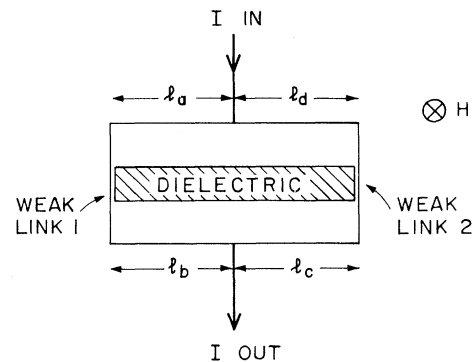


FIG. 1. Schematic diagram of the double-junction interferometer used to measure the penetration depth. Two superconducting films are separated by a dielectric film and joined at the edges of the dielectric by superconducting weak links.

circulating current, B is the applied magnetic field, S is the cross-sectional area of the dielectric hole, and φ_{sc} is the flux due to the penetration of the field into both films. The first integral of Eq. (1) can be written more explicitly as

$$c\Lambda \oint \vec{j}_s \cdot d\vec{l} = c\Lambda(j_a l_a + j_b l_b - j_c l_c - j_d l_d) + (\Delta\theta_1 - \Delta\theta_2) \varphi_0 / 2\pi, \quad (4)$$

where $\Delta\theta_1$ and $\Delta\theta_2$ are the phase changes across weak links 1 and 2, respectively; j_k is the current density in film k ($k = a, b, c, d$); and l_k is the current path length in film k .

It is convenient to distinguish between three contributions to the total current in the superconductor on the basis of their different sources:

(i) screening currents responsible for the Meissner-Ochsenfeld²⁰ effect, (ii) the bias current used to measure the sample critical current, and (iii) a circulating current to satisfy the phase-coherence requirements for the superconducting loop. It will be argued below that the screening currents are zero in the center of the film, so by taking the integral contour to pass through the film centers, the bias and circulating currents comprise the only contributions to the current term in Eq. (4). For the dimensions of the samples used in this experiment, the phase shift $c\Lambda j_k l_k / \varphi_0 \approx \frac{1}{10} \pi$ at $T = 0$ K; for higher temperatures this term increases due to the increase in Λ . In general $j_a l_a + j_b l_b \neq j_c l_c + j_d l_d$ so that the phase change due to these currents must be considered. For now, however, this term will be ignored and the only significant phase changes are assumed to be across the weak links. Equation (4) will therefore be taken to be

$$c\Lambda \oint \vec{j}_s \cdot d\vec{l} = (\Delta\theta_1 - \Delta\theta_2) \varphi_0 / 2\pi. \quad (5)$$

Substitution of Eqs. (2) and (5) into the flux-quantization condition, Eq. (1), gives

$$(\varphi_0 / 2\pi) (\Delta\theta_1 - \Delta\theta_2) + \varphi = n\varphi_0 \quad (6)$$

or

$$\Delta\theta_1 - \Delta\theta_2 + 2\pi(\varphi / \varphi_0) = 2\pi n.$$

1. Josephson Junctions

When the weak links are Josephson junctions the total current through the two junctions in parallel is given by

$$I = I_1 \sin\Delta\theta_1 + I_2 \sin\Delta\theta_2, \quad (7)$$

where I_1 and I_2 are the currents through junctions 1 and 2, respectively. Maximizing I in Eq. (7) subject to the constraints of Eqs. (2) and (6) fully specifies the critical current of the junction pair as a function of the external field.

2. Two Identical Josephson Junctions

The supercurrent through a Josephson junction²¹ in the presence of an applied magnetic field is

$$I = I_{10} \left| \frac{\sin(\pi\varphi_1 / \varphi_0)}{\pi\varphi_1 / \varphi_0} \right| \sin\Delta\theta_1, \quad (8)$$

where φ is the flux enclosed within the effective cross-sectional area of the junction, which for the present rectangular geometry is $\varphi_1 = B(2\lambda + d)w$. Here B is the external magnetic field, w is the width of the junction perpendicular to the field, d is the thickness of the oxide, and λ is the penetration depth of the field into the superconductor on each side of the junction. This result shows that the critical current of the junction is modulated by an externally applied field. Typically $w \approx 0.01$ cm and $2\lambda + d \approx 10^{-5}$ cm, so the modulation field is on the order of 1 G. This single-slit diffraction type of modulation by the magnetic field was first observed by Rowell.²²

The critical current of two identical Josephson junctions in parallel, where it is assumed that the circulating current in Eq. (2) can be ignored, i.e., that $Li_c \ll \phi_0$, is given by

$$I_{\text{crit}} = 2I_{10} \left| \frac{\sin(\pi\varphi_1 / \varphi_0)}{\pi\varphi_1 / \varphi_0} \right| \cos \left[\pi \left(\frac{\varphi_e}{\varphi_0} - n \right) \right] \quad (9)$$

and is periodic in the applied field with a modulation envelope of the form $(\sin x)/x$, an effect first observed by Jaklevic *et al.*²³ For a two-junction loop with an area of 1.0 cm² the field period will be on the order of 10⁻⁷ G, while the period of the amplitude modulation might be as large as 1 G.

3. Unequal Josephson Junctions

When the junctions are not identical, a simple expression analogous to Eq. (9) cannot be obtained for the critical current of the double-junction loop. Also, in general, there will be net circulating current around the loop which cannot be ignored. The critical current of the junction pair for a given value of externally applied flux results from the simultaneous solution of the following equations²³⁻²⁵:

$$I_{\text{crit}} = \{ I_1^2(\varphi_1) + I_2^2(\varphi_2) + 2I_1(\varphi_1)I_2(\varphi_2) \cos[2\pi(\varphi/\varphi_0 - n)] \}^{1/2}, \quad (10a)$$

$$\varphi = \varphi_e + LI_c, \quad (10b)$$

$$I_c = \frac{I_1^2(\varphi_1) - I_2^2(\varphi_2)}{2I_{\text{crit}}}. \quad (10c)$$

Here the expression (10c) for the circulating current assumes that the total current through the junctions is equal to the critical current and

$$I_1(\varphi_1) = I_{10} \left| \frac{\sin(\pi\varphi_1 / \varphi_0)}{\pi\varphi_0} \right|. \quad (11)$$

If the magnetic field dependence of $I_1(\varphi_1)$ and $I_2(\varphi_2)$ can be neglected, it follows from Eqs. (10) that the critical current of the junction pair will oscillate with a period φ_0 as the applied flux

through the loop is increased. Since I_1 and I_2 are assumed constant with field, I_{crit} will have a constant maximum value whenever the total flux in the loop, φ , is an integral number of flux quanta.

From Eq. (10a), I_{crit} will have a constant maximum value whenever $\varphi = n\varphi_0$, and therefore from Eq. (10b) when φ increases from $n\varphi_0$ to $(n+1)\varphi_0$, the external flux φ_e must increase by φ_0 , thereby establishing the strict periodicity of I_{crit} with a change φ_0 in φ_e .

Equations (10) can be solved numerically to find the magnitude of the modulation of the critical current if the values of I_1 , I_2 , and L are known. In general the experimental situation is more complex than the situation considered thus far. The current leads to the two-junction loop may not be symmetrically placed, and the inductance of the two paths through the junctions will not be equal, contrary to assumptions implicitly made above. Although this additional flux complicates the task of obtaining a realistic solution, it does not alter the basic conclusion about the period of the flux quantization. In this regard Fulton²⁶ has recently given an interesting graphical method of investigating the nature of the solutions of nonsymmetrical two-junction loops.

If, however, we also include the dependence of I_1 and I_2 upon the magnetic flux in the junctions, then unless the junctions are identical, the critical current will not be exactly periodic with a change of φ_0 in the applied flux. Equation (10a) indicates that the sample critical current will be a maximum whenever $\varphi = n\varphi_0$, but with the magnitude of I_1 and I_2 a function of the applied magnetic field, the maxima of I_{crit} will not be constant but will also be a function of the applied field. Further, i_c will not have constant minima whenever $\varphi = n\varphi_0$ because I_{crit} has a field dependence, and the field dependence of I_1 and I_2 will cause their relative values to change. Therefore as the total flux changes from $\varphi = n\varphi_0$ to $\varphi = (n+1)\varphi_0$, there will be a small change Δi_c in i_c (which will be positive or negative depending upon how the relative values of I_1 and I_2 change) so that the change in external flux necessary to change the total flux φ by φ_0 is $\varphi_0 - L\Delta i_c$. Only if $I_1 = I_2$ and both are independent of applied field will the total critical current be periodic with applied flux with exactly a period of φ_0 . This effect has not been previously noted, and it can have considerable importance for high-precision measurements of the absolute value of magnetic flux²⁷ or current.²⁸

To estimate the magnitude of the nonperiodicity, denote the effective cross-sectional areas of the two junctions and the loop by S_1 , S_2 , and S_l , respectively (i. e., $\varphi_1 = BS_1$, etc.), and write

$$I_{20} = \alpha I_{10}, \quad S_2 = \beta S_1, \quad S_l = k S_1.$$

When the flux within the loop is increased from zero to one flux quantum, from Eq. (2) the flux from the externally applied field must change by

$$\varphi_e(\varphi_0) - \varphi_e(0) = -\varphi_0 - L[i_c(\varphi_0) - i_c(0)].$$

Assume $\varphi_1 \ll \varphi_0$, $\varphi_2 \ll \varphi_0$, and that the current flowing through each junction is the critical current. Then the circulating current can be calculated from Eq. (10c), and we find

$$\varphi_e(\varphi_0) - \varphi_e(0) \approx \varphi_0 \pm L I_{10} \left(\frac{\pi^2}{3} \right) \left(\frac{1 - a^2 \beta^2}{1 + a} \right) \left(\frac{1}{k^2} \right). \quad (12)$$

[The particular set of coefficients shown in Eq. (12) was obtained by using Eq. (11).] When the critical current goes through a complete period (φ increased by one flux quantum), the externally applied flux increases by slightly less (or more) than φ_0 . For the present experiments it was found that the measured period in the applied magnetic field could vary as much as 12% over small field increments. The example of Fig. 2 has a variation of 8%. This agrees with a theoretical estimate based on Eq. (12) for this sample of $\pm 4\%$.

The nonperiodicity caused by the field dependence of the critical currents can be partially avoided. Reversing the magnetic field direction and averaging the results should eliminate the effect. In practice, however, flux locked in the junctions to an unknown and irreproducible extent limits the value of this procedure. Counting voltage oscillations between points at which the voltage is zero or at least equal is a useful way of decreasing the nonperiodic effect, but it does not eliminate it unless the field dependence of the critical current of the two junctions is the same. With other experimental arrangements the breakdown in periodicity is not nearly as severe as in the case considered above. With point contacts the loop-to-junction area ratio can be greatly increased, and it is also possible to adjust the value of the critical current. These factors can reduce the nonperiodicity to the neighborhood of one part in 10^6 .

In practice the period was determined by dividing the magnetic field increment by the number of critical-current maxima in that increment. If $I_1(\varphi_1)$ and $I_2(\varphi_2)$ have the same value at the final magnetic field H_f as they did at the initial field H_i , the circulating current will be the same at the end points and the average period will be exactly φ_0 over the properly chosen field interval. Unfortunately, it is usually not possible to tell when both I_1 and I_2 have returned to an initial value as the external field is varied, because they are in parallel and are not measured separately. In addition, their exact field dependence is not known. Experimentally the best procedure is to average the peri-

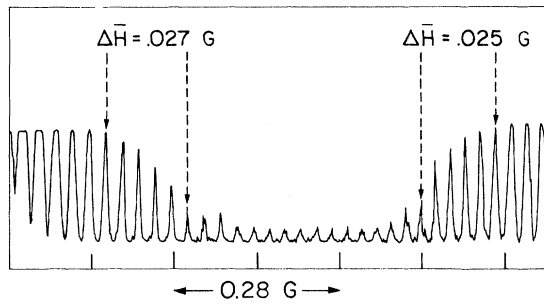


FIG. 2. Voltage vs magnetic field for sample 286 (see Sec. IV for description of the sample) with sample biased with a constant current. The change in the average magnetic field period is due to the field dependence of the junction's critical current.

od over as many complete periods of the modulation of I as is practical.

In the previous discussion the phase contribution $c\Lambda \int \vec{j}_s \cdot d\vec{l} 2\pi/\phi_0$ from the currents in the films was dropped from the fluxoid-quantization condition, although it was noted that the term is not always small. With its inclusion, Eq. (6) becomes

$$\Delta\theta_1 - \Delta\theta_2 = 2\pi \left(\frac{\varphi}{\phi_0} + \frac{c\Lambda}{\phi_0} (j_a l_a + j_b l_b - j_c l_c - j_d l_d) - n \right),$$

and the expression on the right-hand side of this result is the argument of the cosine in Eq. (10a). The period of the sample critical current with magnetic field will not be affected by this additional term if the current distribution in the sample is the same whenever the critical current has its maximum value. But for nonidentical junctions the circulating current changes slightly as each flux quantum is added, so the current distributions will be slightly different at each maximum in the critical current. The phase change from the redistributed current densities in the loop will add to the fluxoid in the same sense that the change in i_c does and will enhance the deviation of the periodicity.

4. Metallic Weak-Link Junctions

Josephson's original calculation was for tunneling through a thin oxide barrier, but a variety of connections between two superconductors have been used which give results similar to an oxide junction. These include point contacts,²⁹ narrow constrictions in thin films,³⁰ and a normal-metal barrier between two superconductors.³¹ Double-junction interference effects have been seen in samples consisting of two Nb wires pressed together³² and between a Nb wire and a blob of Sn-Pb solder melted around it.³³

Both Josephson²¹ and Anderson³⁴ have shown that a necessary requirement to obtain Josephson

phase-coherence effects is that at some connecting point in the superconductor the magnitude of the order parameter is greatly reduced, resulting in a low critical current at that point. At the constriction there is a high current density causing a rapid phase change across it. An important difference between oxide junctions and point contacts for this experiment is that the current-phase relation for an oxide junction, $j = j_0 \sin\Delta\theta$, is not obeyed for weak links. Schwartz and Baratoff³⁵ have shown by analyzing Zimmerman and Silver's³⁶ experiment (in which the flux contained in a superconducting loop broken by one point contact was measured) that the current-phase relationship for weak links is not the simple sinusoidal one that holds for an oxide junction. However, the periodic dependence of the current on the phase, modulo 2π , remains.

The relation $j = j_0 \sin\Delta\theta$ has been used to derive Eqs. (10). Although these equations do not exactly describe superconducting weak links, the periodicity in the current-phase relation leads to similar periodicity in the measured critical current. Thus, for two weak-link junctions, the critical current of the junction pair will still be periodic in the applied field; however, if the two junctions are not identical, the period will, as before, not be exactly ϕ_0 . Often in practice a point-contact junction is actually a collection of several contacts closely spaced. The currents through the different contacts will interfere and can produce a complex interference pattern. The basic flux period corresponding to the loop with the largest area of contact will be modified by the coherent additions of other loops with different periods. If the various periods are incommensurate, there will be no obvious periodicity with magnetic field, although there will be a definite modulation pattern.

5. Resistive Superconducting State

In this experiment the periodicity in the critical current of the two weak-link samples is not measured directly. Instead the sample is biased with a constant current that is just larger than the critical current so that a small voltage appears across the junctions. To produce this voltage a small normal current flows across each junction. The supercurrents are at their critical values and are not affected by the normal current, and their response to a magnetic field is that described above.³⁷ Since the critical supercurrent is modulated by an applied field, whereas the total current remains constant, the normal component of the current is also modulated by the field resulting in a modulation of the output voltage. When the critical current is a maximum, the voltage will be a minimum, and as the field is increased, the critical current falls, and the voltage increases. The minimum in

critical current corresponds to a voltage maximum. The voltage will exhibit the same magnetic field period as the critical current, at least in the limit of zero voltage.

To account for the normal currents through the junctions, Eq. (10b) for the circulating current must be modified. Write the current through each junction as

$$i_k = i_{kS} + i_{kN} = I_k(\varphi_k) \sin \Delta \theta_k + i_{kN}, \quad k = 1, 2$$

where

$$i_{kN} = V/R_k.$$

In general, $R_k = R_k(V, \Delta \theta_k)$. When the junction is an oxide film, the normal current will be very similar to the usual single-particle tunneling current.³⁸ The normal current will be very low for voltages less than twice the energy gap of the superconductor (assumed the same on each side of the oxide), and at voltages higher than twice the gap the current rapidly approaches the value V/R_N , where R_N is the normal-state resistance of the junction.³⁹ For metallic weak links the situation is more complicated. The total current in the sample is given by $i = i_1 + i_2$, and the total circulating current is then

$$\begin{aligned} i_c &= \frac{1}{2}(i_1 - i_2) = \frac{1}{2}(i_{1S} - i_{2S}) + \frac{1}{2}(i_{1N} - i_{2N}) \\ &= I_c + \frac{1}{2}(i_{1N} - i_{2N}), \end{aligned} \quad (13)$$

where Eq. (10c) is the appropriate expression for the circulating supercurrent. Since the junctions are in parallel, the normal current must also satisfy

$$V = i_{1N}R_1 = i_{2N}R_2. \quad (14)$$

If we consider two identical Josephson junctions, the normal current through each junction is the same, and we arrive at

$$V = R_1 \left[\frac{1}{2}i - I_1(\varphi_1) \cos(2\pi\varphi_1/\varphi_0) \right]. \quad (15)$$

Since the sample is biased with a constant current source i the voltage is periodic in the applied field with period φ_0 . The modulation of the junction critical current with field gives a modulation envelope of the voltage with a larger field period.

When the two junctions are not equal, it turns out as before that additional errors in determining the number of flux quanta can arise from the circulating normal current. However, this source of error can be avoided by restricting the bias current so that the voltage is zero at the initial and final field points.

B. Flux Penetration in Thin Films

The solution of the electrodynamic equations relates the penetration depth λ to the flux penetration into the film. Both lead and tin, the materials used in this experiment, are nonlocal supercon-

ductors. However, the solution for the field penetration into a film is very difficult in the nonlocal case and has been found for only a few special cases.⁴⁰ Since many results obtained from the local theory apply with only quantitative changes in the nonlocal case we consider first the local limit and later consider the way in which this analysis must be modified in the nonlocal theory.

1. Local Theory

In the London local theory the magnetic field distribution in a superconductor is determined by the equation

$$\nabla \times \nabla \times H = - (1/\lambda_L^2)H, \quad (16)$$

where $\lambda_L^2 = \Lambda c^2/4\pi$. Assume a magnetic field is applied in the z direction parallel to the surfaces of a thin film of thickness d with the surfaces at $x = \pm \frac{1}{2}d$ and of infinite extent in the y and z directions. Equation (16) then reduces to

$$\frac{d^2 H_z}{dx^2} - \frac{H_z}{\lambda^2} = 0. \quad (17)$$

When the applied field on both sides of the film is H_1 the field distribution within the film is

$$H_z = H_1 \frac{\cosh(x/\lambda)}{\cosh(d/2\lambda)}, \quad (18)$$

and the current distribution is

$$j_y = - \frac{c}{4\pi} \frac{\partial H_z}{\partial x} = \frac{cH_1}{4\pi\lambda} \frac{\sinh(x/\lambda)}{\cosh(d/2\lambda)}. \quad (19)$$

The above result is modified if the field is not equal at the two surfaces. The general solution of Eq. (17) with unequal fields H_1 and H_2 at the two surfaces is

$$H_z = \frac{(e^{d/2\lambda}H_2 - e^{-d/2\lambda}H_1)e^{x/\lambda} + (e^{d/2\lambda}H_1 - e^{-d/2\lambda}H_2)e^{-x/\lambda}}{2 \sinh(d/\lambda)}. \quad (20)$$

If we now increase each of the applied fields by the same amount ΔH so that

$$H'_1 = H_1 + \Delta H, \quad H'_2 = H_2 + \Delta H,$$

the new field distribution can be written as

$$H'_z = H_z + \Delta H \frac{\cosh(x/\lambda)}{\cosh(d/2\lambda)}. \quad (21)$$

The additional fields in the film caused by the increase ΔH at both boundaries have the same distribution as given in Eq. (18).

This solution is applicable to the samples used in this experiment. As indicated in Fig. 1, two parallel films are joined by superconducting weak links. During the measurement the weak links are in the critical state and thus provide no barrier to flux penetration. From Eq. (3) the internal field in the hole of the sample will differ from the ex-

ternal field at the outer surface by the contribution from the circulating current. Since the circulating current is periodic with field, as the external field is increased there will be a succession of field values at which the internal and external fields satisfy Eq. (21) with ΔH equal to the field period of the circulating current. Hence the field increment ΔH has a distribution within the film given by Eq. (18), and, in particular, from Eq. (19) the current density induced by this field is zero at the center of the film. This argument assumes that λ is not dependent upon H or j , and is not affected by the difficulty discussed above in measuring the period of the circulating current.

The Ginzburg-Landau (GL) local theory uses the same equation as the London theory [Eq. (16)] to determine the magnetic field distribution, but λ is a function of H and T to be determined self-consistently to minimize the free energy. It is expected that deviations from London electrodynamics would be confined to a region quite close to the phase transition and to only those films that are thin enough to lead to a second-order phase transition.

For the configuration of Fig. 1 the path of integration for the fluxoid-quantization condition, Eq. (1), is taken through the center of each film where the current density induced by the external field increment ΔH is zero. The additional contribution to the fluxoid is the flux contained within the path

$$\begin{aligned} \Delta\varphi_e &= \oint \Delta\vec{A} \cdot d\vec{l} = \int \Delta B dS \\ &= \mu \Delta H w \left(d + \lambda_1 \tanh \frac{d_1}{2\lambda_1} + \lambda_2 \tanh \frac{d_2}{2\lambda_2} \right), \end{aligned} \quad (22)$$

which we may write

$$\Delta\varphi_e = \mu \Delta H w (d + \delta_1 + \delta_2), \quad (23)$$

where

$$\delta_i = \lambda_i \tanh(d_i/2\lambda_i), \quad (24)$$

when the modulation of the critical current by the applied magnetic field has period φ_0 in φ_e :

$$\varphi_0 = \Delta\varphi_e = \mu \Delta H w (d + \delta_1 + \delta_2). \quad (25)$$

A measure of the field increment between successive maxima in the sample critical current determines the flux penetration into the two films when the dimensions of the hole (d and w) are known.

2. Nonlocal Theory

Schrieffer⁴¹ has calculated the magnetic susceptibility of a film in a field parallel to its surface for the Pippard kernel and found that deviations from the London theory given above occur for a film thickness less than twice the penetration depth and give a susceptibility smaller than the London value.

Measurements of critical-field data for thin films^{42,43} have been analyzed by substituting for λ in the GL expression for the critical field

$$H_c = (\sqrt{24}) (\lambda/d) H_{cb}, \quad (26)$$

a thickness-dependent penetration depth λ_d that accounts for the nonlocal effects. Here H_{cb} is the critical field of the bulk material and d is the thickness of the film.⁴⁴ Ittner⁴⁵ calculated the field distribution in a thin film using Schrieffer's result for the susceptibility and found the distribution could be well approximated by a London type of distribution with λ_L replaced by a thickness-dependent λ_d ; λ_d is determined by equating the London susceptibility to Schrieffer's nonlocal value. Toxen⁴² calculated λ_d in this way and found very close agreement between the theoretically predicted critical field and his experimental data. Thompson and Baratoff⁴⁶ discuss the conditions under which such a replacement is valid and give an explicit expression for λ_d on the basis of their microscopic nonlocal theory of thin films in magnetic fields.

III. EXPERIMENT

A. Sample Description

To measure the flux penetration into a superconducting film it was necessary to fabricate a doubly connected sample with two junctions in parallel as schematically indicated in Fig. 1. It was desirable that the junction material have a higher critical temperature and critical field than the sample film so that the junction properties would not change significantly while the temperature or applied magnetic field were varied during the course of an experimental run. In addition, it was useful to have the junctions made in the form of very narrow superconducting weak links, or shorts, so that they would have a high critical field and measurements could be made at comparatively large values of magnetic field. To satisfy these requirements, tin was used for the sample film and the junctions were made with lead.

Weak-link junctions were formed by fabricating Pb-PbO-Pb tunnel junctions and then letting the junctions anneal at room temperature until the oxide was shorted, due either to Pb or O migration. This shorting process usually took place within a time which varied from 2 h to 1 day and always occurred if the original oxide was not too thick.

An end view of the actual sample used is shown in Fig. 3. The sample film was first evaporated onto the glass substrate, then the dielectric (SiO) "hole" of the loop was evaporated, next two Pb strips were evaporated so that they passed over the edge of the dielectric to make contact with the

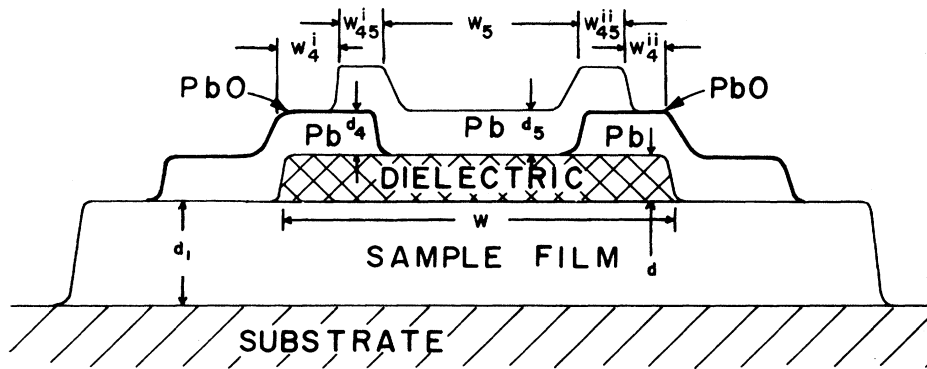


FIG. 3. End view of sample used to measure the penetration depth.

sample film; these Pb strips were oxidized and the superconducting loop was then completed by evaporating a final Pb strip that overlaps the first two Pb strips. The junctions are the regions of overlap of the Pb films.

B. Sample Preparation

The sample was fabricated by seven successive evaporations using standard techniques in an oil-diffusion-pumped vacuum system. The bell jar enclosed an Allen-Jones Carrousel mask changer,⁴⁷ which allowed one to choose independently from six different substrates, masks, and source materials.

The sample preparation required more evaporations than there were masks in the changer, so the vacuum was broken once during the sequence of evaporation in order to change the masks.

The usual sequence of evaporation was as follows (the numbers in parentheses refer to the order of evaporation of the various films as labeled in Fig. 4). First, a long rectangular film of the sample material (1), Sn or Pb, was evaporated; this film was 5 mm wide and extended most of the substrate length. Then a smaller rectangle of SiO (2) was centered on top of the sample film and formed the dielectric core of the sample; the SiO was approximately 2 mm wide and 1500 Å thick. Next SiO sections (3) were deposited that extended from the central SiO piece to the edge of the sample film; these films were sufficiently thick and wide to provide insulation for Pb strips to be evaporated later. The appearance of the sample thus far is shown in Fig. 4(a). Generally at this point the vacuum was broken, and the masks were changed.

The fourth evaporation formed the two narrow Pb cross strips (4) that are perpendicular to the SiO strip (2) and cross over the sides of it to make contact with the sample film (1); these strips were about 0.2 mm wide, 2 mm long, and 1500 Å thick. These Pb films were then oxidized by a glow discharge in a manner to be described below. Next a

rectangular Pb film (5) 1500 Å thick, 1.5 mm wide, and 4.5 mm long was evaporated parallel to the sample film. Each side of the Pb film (5) covered the ends of the Pb cross strips (4), and these overlap areas comprised the junctions. Figure 4(b) shows the sample at this stage.

Finally, strips of Pb (6) were evaporated to provide access to strip (5) so that a four-terminal network was made to each junction; these strips were 1.5 mm wide and thick enough to be electrically continuous over the various steps in film thickness. The final evaporation formed the solder terminals (7) at the ends of films (1) and (6). A top view of the completed sample is given in Fig. 4(c).

The substrate was at room temperature for all evaporations except for that of the Sn. For Sn the substrate was cooled to liquid-nitrogen tempera-

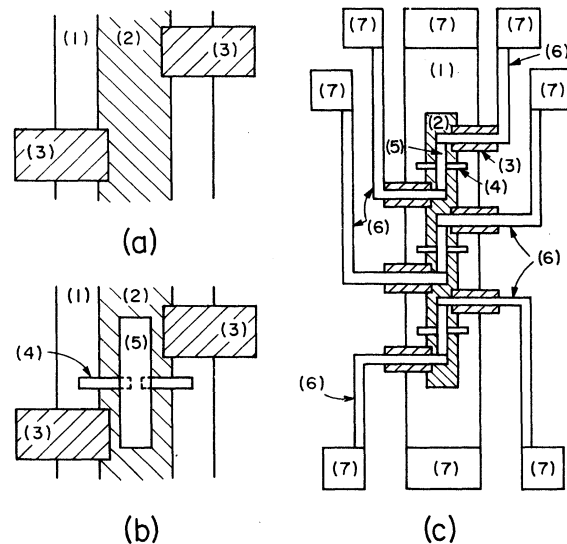


FIG. 4. (a) and (b) are successive stages in the sample evaporation; (c) is the top view of the completed sample. Details of the evaporation procedure are given under sample preparation.

ture by raising the mask and substrate assembly firmly against a copper cup filled with liquid nitrogen. The specially modified substrate holder had clips to hold the substrates against a $\frac{1}{4}$ -in. -thick piece of copper. When the substrates were raised, this piece of copper was pressed directly against the copper bottom of the liquid-nitrogen cup. As indicated in Fig. 5 the liquid-nitrogen cup was made with a flexible metal bellows to allow its bottom to make good contact over the entire area of the substrate holder.

The metals were evaporated at an initial pressure in the neighborhood of 10^{-7} mm Hg; the pressure during the evaporation usually remained below 5×10^{-7} mm Hg, although on occasion it rose to 10^{-6} mm Hg. The metal films were evaporated in from 20 to 40 sec.

The SiO films were evaporated more slowly in a poor vacuum; the rate was approximately $5 \text{ \AA}/\text{sec}$ with a vacuum of $5\text{--}10 \times 10^{-5}$ mm Hg. Initially the low vacuum was achieved by partially or completely closing the slide valve between the diffusion pump and the bell jar, but with later samples a small flow of dry O_2 was admitted, and the slide valve was kept just barely open. A Drumheller⁴⁸ SiO source was used. This procedure usually produced insulating SiO coatings.

The Pb film was oxidized by exposure to an oxygen glow discharge.⁴⁹ The substrate was above the cathode and shielded from direct exposure to cathode emission by an aluminum sheet. One mask holder was removed from its turret, and this hole was positioned between the film and the cathode during the discharge. The glow discharge was operated at a voltage of 0.5 or 0.6 kV with currents in the range 20–50 mA. The O_2 pressure was about 0.1 mm Hg.

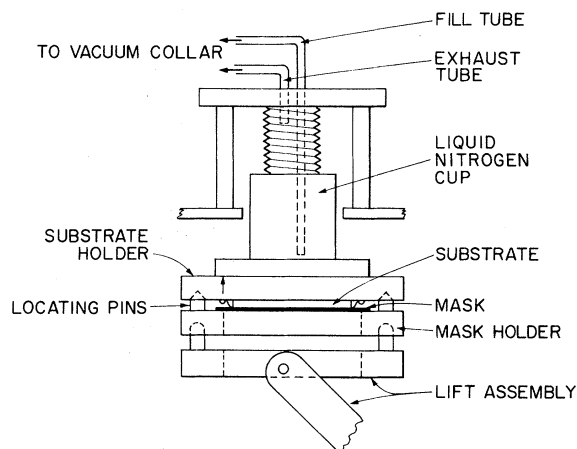


FIG. 5. Details of the substrate cooler, the mask, and substrate assembly.

C. Experimental Apparatus

The glass substrate was mounted in a phenolic holder at the end of the cryostat insert. The substrate holder could be tipped in two mutually perpendicular directions, one perpendicular and one parallel to the plane of the film. The tipping was accomplished by rotating threaded rods that extended down from the top of the cryostat.

For magnetic field measurements on thin superconducting films it is essential that the field be parallel to the plane of the film. The film was aligned by applying a magnetic field sufficient to put the film into the transition region and then tipping the film perpendicular to its plane until a minimum value of the film resistance was found. The angular position of the film determined in this manner was repeatable to within 4×10^{-3} rad.

The cryogenic apparatus consisted of two concentric glass liquid-helium Dewars surrounded by a liquid-nitrogen Dewar. The outer helium Dewar contained the superconducting magnet. The whole assembly was surrounded by a magnetic shield to attenuate the earth's field and other stray fields.

The pressure of the helium vapor in the sample Dewar was controlled by a diaphragm manostat at temperatures above the λ point of liquid helium and by an electronic regulator⁵⁰ at lower temperatures. The temperature was determined from the pressure of the helium vapor with corrections, when necessary, for the height of the liquid above the sample. Below the λ point of helium (2.17 K), the temperature was determined from the resistance of a 10- Ω Allen-Bradley $\frac{1}{2}$ -W resistor which has the property that a plot of the logarithm of the pressure as a function of the logarithm of the resistance is a straight line at temperatures below the λ point.⁵¹

A 20-kG superconducting magnet wound in this laboratory from a NbTi alloy was mounted on the outer wall of the sample Dewar. The magnet has compensating end windings to give maximum homogeneity to the field near the center of the magnet.⁵² The axial field deviated from the maximum value by 0.1%, $\frac{3}{8}$ in. from the magnet center and by 1%, 1 in. from the center.

The magnet had an additional feature. To do the experiment as a function of magnetic field it was necessary to have a very stable source for the applied field in addition to the small field which was swept to observe the flux-quantization periods. A superconducting magnet in the locked-in mode was the obvious choice for the large applied field. To sweep the field over a small range, the main coil was wound in two sections. The first section was a conventional magnet, while the second section consisted of additional windings on the same coil form that enclosed secondary windings. When cur-

rent passed through the secondary windings, the flux in this section of the main coil was changed, and since the flux within the entire main winding had to be conserved (with the magnet operated in the locked-in mode) the flux in the large section changed in the opposite direction. Thus a current through the secondary windings caused a change in field in the main coil. Figure 6 is a schematic diagram of the coil configurations.

D. Experimental Procedure

The resistance of the two parallel junctions was measured with a four-terminal network. It usually took 30 min to finish the evaporation and measure the sample resistances after the Pb strip (5) had been evaporated to complete the junctions. If the junction resistance was greater than 1000 Ω , the sample then became a candidate for further investigation. If the resistance was tens of ohms or less, the sample was rejected.

For those samples with high resistances, the resistance was monitored until it fell into the range 10–20 Ω . This shorting of the junction usually took place within 1 day. Next the resistance of the sample film [film (1) in Fig. 5] was measured, and then the sample holder was inserted into the Dewar, which had been kept at liquid-nitrogen temperature so the sample would be quickly cooled in order to prevent further changes in the junctions.

The current-voltage (I - V) characteristic of the superconducting junctions was then traced. In all successful samples the I - V curve of the junction had the step structure that is characteristic of weak-link junctions.^{37,53}

To see if the sample voltage would exhibit flux-quantum periodicity, the sample was biased with a

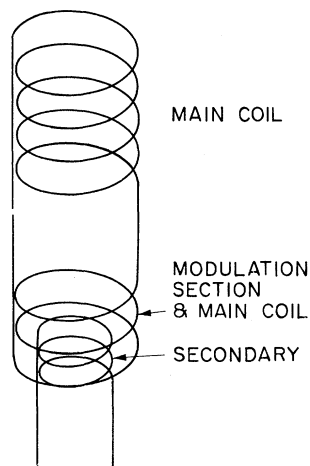


FIG. 6. Schematic diagram of the magnet windings to indicate how the field from the main coil is modulated by a current through the secondary coil.

constant current slightly larger than the critical current, and the magnetic field was slowly varied. If the sample passed this final test, the junction voltage versus the magnet current was traced on an X - Y recorder for different values of temperature and magnetic field.

Figure 7(a) is a trace of the junction voltage as a function of magnetic field for one of the Pb samples. This sample was unique in that only one setting of the bias current was necessary to obtain the complete magnetic field information. This sample beautifully exhibits the two field periods discussed in Sec. II; namely, the smaller period in the sample critical current due to the requirement of phase coherence around the total superconducting loop and the larger period of the envelope due to the modulation of the critical current of each junction. For other samples the modulation amplitude of the envelope was so large that it was not possible to obtain continuous traces of the small-period oscillations at one bias setting. This situation is illustrated in Fig. 7(b). At low values of the bias, the critical current is not reached for a certain range of field, and there are thus no voltage oscillations for this range (lowest curve). Increasing the bias until we obtain periodicity for this range of field may cause the upper portion to fall on the first voltage step of the I - V curve and show no oscillations. On such a step the voltage is independent of current, an effect which is presumably caused by a geometrical resonance, where the voltage is determined by the resonant frequency according to the Josephson relation $2eV = h\nu$. By taking several field sweeps at different bias currents it was possible to get the total count of the number of oscillations in a given field increment. The period obtained in this manner was never observed to depend on the value of the bias current as long as $V=0$ at the magnetic field end points.

Frequently the curves had structure at values of the field corresponding to one-half the period. When curves had been obtained in which there was no ambiguity about which voltage minima corresponded to flux-quantum periods, the data were analyzed by dividing the total number of periods within the field increment by the value of the field increment. The average field period ΔH obtained in this manner is the value of magnetic field necessary to add one flux quantum to the loop. When the period of the modulation envelope of the sample critical current was obvious, ΔH was determined from the average over three or four complete periods of the amplitude modulation.

IV. RESULTS

The dimensions of the samples used in this experiment are given in the Table I. All film thick-

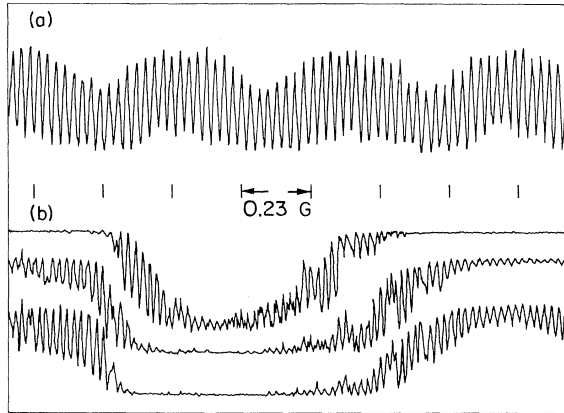


FIG. 7. Voltage-magnetic-field curves for two different samples.

nesses were measured by a multiple-beam interferometer using the method of equal chromatic order.⁵⁴ For those films whose thickness was measured more than five times, the standard deviation of the measurements was in the neighborhood of 50 Å. All film thicknesses were measured at least three times.

To analyze the experimental results, Eq. (25) must be modified since the top Pb films overlap. Referring to Fig. 4(c), let w_4 be the width of the portion of film (4) that is not covered by film (5), let w_5 be the width of the portion of film (5) that does not cover film (4), and let w_{45} be the width of the overlap of films (4) and (5). Also, let d_4 and d_5 be the thickness of films (4) and (5), respectively, and let $d_{45} = d_4 + d_5$, then Eq. (25) becomes, using Eq. (24),

$$\varphi_0 = \mu \Delta H w \left[d + \lambda_1 \tanh \frac{d_1}{2\lambda_1} + \lambda_{Pb} \left(\frac{w_4}{w} \tanh \frac{d_4}{2\lambda_{Pb}} + \frac{w_5}{w} \tanh \frac{d_5}{2\lambda_{Pb}} + \frac{w_{45}}{w} \tanh \frac{d_{45}}{2\lambda_{Pb}} \right) \right], \quad (27)$$

where d_1 is the thickness of the sample film, d is the thickness of the SiO film, and w is the width of the SiO film, $w = w_4 + w_5 + w_{45}$.

A. Pb Samples

Of the samples composed entirely of Pb films two behaved in accordance with the description of Sec. II. Several other measured samples had an erratic amplitude modulation of the critical current as a function of magnetic field. The results from these latter samples are not reported here since it was not possible to correctly determine the period from the observed modulation pattern. It is probable that the number and distribution of shorts in the junctions gave these samples a very complex pattern without obvious periodicity.

TABLE I. Dimensions of the samples used. Symbols are defined in Fig. 3.

Sample	Sample film	w (mm)	w_4 (mm)	w_5 (mm)	w_{45} (mm)	d (Å)	d_1 (Å)	d_4 (Å)	d_5 (Å)
302	Pb	2.50	1.23	0.61	0.66	1800	1630	1560	1660
319	Pb	2.50	1.23	0.61	0.66	1470	2390	1290	1150
286	Sn	2.51	1.24	0.61	0.66	1600	2830	1550	1100
340	Sn	2.50	1.24	0.62	0.64	1700	2090	1600	1290

1. Absolute Value of λ

Using the measured values of the film thickness Eq. (27) was solved for λ_{Pb} ; λ was assumed to be equal for all films in the sample. The values of λ_0 , that is, λ at $T=0$ [more precisely, at $T=2$ K which corresponds to $t=0.29$ and $Y=1.003$, where $t=T/T_c$ and $Y=(1-t^4)^{1/2}$ for an assumed critical temperature of 7.2 K for the Pb films] for the two Pb samples are given in Table II.

The error quoted for sample 302 is the error in λ from the estimated error in the measurement of the thickness of the SiO film. The error in λ from the error in the period determination is much smaller than 50 Å. Sample 302 exhibited a clear modulation envelope of the maximum critical current, and the period of the critical current was well defined; the beautiful pattern obtained from this sample is shown in Fig. 7(a).

While the value for λ obtained from sample 319 agrees with that from sample 302 within the experimental error, it was not as good a sample as 302. It had a modulation envelope with a good deal of structure that made it difficult to count the oscillations, and the period obtained at different temperatures varied randomly by a few percent. The value quoted is based on the average value of the period measured at different temperatures (from 4.2 down to 2 K).

The measured value of 630 Å is higher than the BCS predicted value of 480 Å and higher still than the previously accepted experimental value of 390 Å.⁵⁵ Swihart and Shaw⁵⁶ have recently recalculated the theoretical value for Pb and find $\lambda = 406$ Å. Their result differs from Bardeen and Schrieffer's because they use different values for λ_L and the Fermi velocity. In both calculations the nonlocality of Pb is accounted for, but the superconductor is assumed to be a bulk material with an infinite mean free path. (In the discussion to follow the Bardeen-Schrieffer value will be

TABLE II. Measured absolute values of λ_0 , the penetration depth at $T \approx 0$ for two lead films.

Sample	λ_0 (Å)
302	630 ± 50
319	640

used.) However, for the Pb films used in the experiment the mean free path is finite due to impurity scattering and scattering at the film surface. The adjustment of the theoretical value to include the effect of a finite mean free path will raise the value of λ and bring the predicted value closer to the observed value.

If Pb were a local superconductor (which it is close to being since $\xi/\lambda = 2.04$), the mean-free-path correction would be given by the simple relation⁵⁷

$$\lambda(l) = \lambda_L \left(\frac{\xi_0}{\xi(l)} \right)^{1/2} = \lambda_L \left(1 + \frac{\xi_0}{l} \right)^{1/2}, \quad (28)$$

where for Pb $\xi_0 = 760 \text{ \AA}$. The mean free path for Pb at room temperature was determined by comparing the resistivities of Pb and of Sn films that were evaporated through the same mask [film (1) in Fig. 5]. Using the measured values of ρl ,⁵⁸ where ρ is the resistivity and l the mean free path of the material, for Pb and Sn the ratio of their mean free paths can be determined from the ratio of the film resistances. Using 97 \AA as value of the mean free path in Sn⁵⁹ gives 60 \AA for the mean free path at room temperature of the 1500-\AA Pb films used in this experiment.

If Matthiessen's rule is assumed to hold, the mean free path in the residual resistance region is given by

$$l_R = l_{300} \left(\frac{R_{300}}{R_{4.2}} - 1 \right), \quad (29)$$

where R_{300} and $R_{4.2}$ are the film resistances at room temperature and at liquid-helium temperature, respectively. For sample 310 the sample film had a resistance ratio $R_{300}/R_{4.2} = 75.7$ while for sample 316 the ratio was 53.2. The resistance ratio for the sample film of sample 316 will be taken to be typical for 1500-\AA -thick films, and it gives an approximate mean free path of 3000 \AA at 4 K. Substitution of this value into Eq. (28) gives $\lambda_0(l) = 1.12\lambda_0$. This correction raises the theoretical value of λ_0 to 538 \AA . However, this result is only a rough approximation to the correct mean-free-path dependence since Pb is not a local superconductor.

A better correction for the theoretical value of λ in a thin film is contained in the Thompson-Baratoff theory of nonlocal superconducting films.⁴⁶ Their formula for the penetration depth λ_d in a film of thickness d in the limit $d \gg \xi$ is

$$\lambda_d = \lambda \left(1 + \frac{\pi^2}{5} \frac{\xi^2}{d^2} \right)^{1/2} \quad (30)$$

for the case of specular reflection scattering at the surface and

$$\lambda_d = \lambda \left(1 + \frac{9}{8} \frac{\xi}{d} \right)^{1/2} \quad (31)$$

for the diffuse scattering case. These corrections are $\lambda_d = 1.2\lambda_0$ and $\lambda_d = 1.1\lambda_0$ for the specular and diffuse cases, respectively. The total nonlocal correction raises the predicted value by from 10 to 20% depending upon which is the proper boundary condition for the surface scattering.

This nonlocal correction assumes an infinite mean free path. An approximate mean-free-path correction can be obtained by using Eq. (29) with l equal to the mean free path for volume scattering, l_∞ (i. e., the mean free path for a bulk sample of the same material that comprises the film) which is given by⁶⁰

$$\frac{1}{l_R} = \frac{1}{l_\infty} + \frac{3}{8d}, \quad (32)$$

where d is the film thickness and l_R is the mean free path determined by Eq. (29). For both samples 316 and 319 the solution of Eq. (32) gives $l_\infty \approx 15000 \text{ \AA}$, and Eq. (28) then gives $\lambda_0(l) = 1.03\lambda_0$.

The combination of the nonlocal and mean-free-path corrections puts the expected theoretical value $\lambda_d(l)$ in the range $1.13\lambda_0$ to $1.24\lambda_0$ or $542\text{--}595 \text{ \AA}$ which, with the probable experimental error of 50 \AA , is in fair agreement with, although still lower than, the measured value of 630 \AA . Using the Swihart-Shaw result gives a range for the theoretical value of $459\text{--}503 \text{ \AA}$ which is considerably below the measured value.

2. Temperature Dependence of λ

It was possible to measure the temperature dependence of λ in Pb only in sample 302, and the results are given in Fig. 8. In this figure the data are compared with the temperature dependence measured by Erlbach *et al.*⁶¹ They found that their measured temperature dependence agreed with the prediction of the BCS theory if a slightly larger value for the energy gap was used than that determined by the theory. They used $\Delta = 4.93kT_c$ while the BCS theory predicts $\Delta = 3.52kT_c$; the higher experimental value is presumably due to the strong-coupling nature of Pb.

The initial rapid rise of the data is probably spurious and reflects experimental error. The data for $Y > 1.02$ are within 1% of the data of Erlbach *et al.*, and this difference is well within the experimental accuracy. This curve has been normalized to λ_0 and so is not very sensitive to error in the absolute value of λ_0 that arises from the uncertainty in the measurement of the thickness of the SiO film. This sample exhibited the period change discussed in Sec. II and some error in the period determination is expected. However, data were taken over 12 full periods in the envelope modulation, so this error is very small. If the error in the period was on the order of $\frac{1}{2}\%$, the resulting error in λ would be slightly more than 1%

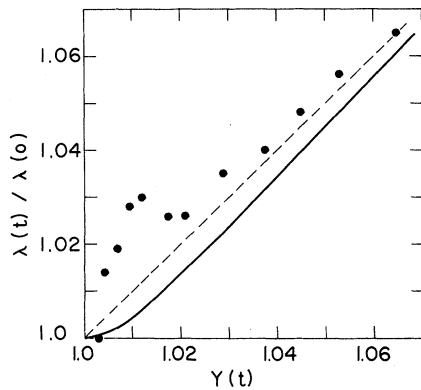


FIG. 8. $\lambda(t)$ as a function of $Y(t) = (1 - t^4)^{-1/2}$ for the Pb films of sample number 302. The solid curve is the measurement of Erlbach *et al.* (see Ref. 61).

(since the change in the period is due only to the change in λ which comprises roughly one-half the area), and so the agreement between the data and those of Erlbach *et al.* is quite satisfactory.

B. Tin Samples

1. Absolute Value of λ

The absolute value of λ_0 was obtained for two Sn samples (at $t = 0.29$ for 286 and $t = 0.30$ for 340) as given in Table III.

Table III includes the mean free paths calculated from Eqs. (29) and (32) using $l_{300} = 97 \text{ \AA}$.⁵³ For each value of mean free path, $2l/\pi\xi_0$ has been calculated in order to compare the results with Miller's⁶² calculation (Table I in his paper), which is given here in Table III. For both samples 630 \AA has been used for the value of the penetration depth of the Pb films in the samples.

The experimental values are in fair agreement with Miller's calculation from the BCS theory. His calculations determine the mean-free-path dependence of λ , but they do not, of course, include the additional nonlocal corrections for the film thickness. Using l_∞ , the Thompson-Baratoff factors from Eqs. (30) and (31) are given in Table

TABLE III. Measured absolute values of λ_0 , the penetration depth at $T \approx 0$, for two tin films compared with theoretical values from Miller (Ref. 64). Mean free path of the film l , calculated from Eq. (32) from the thickness d and the bulk mean free path l_∞ .

Sample	$\lambda_0(\text{\AA})$	$l_R(\text{\AA})$	$\frac{2l_R}{\pi\xi_0}$	$l_\infty(\text{\AA})$	Miller		
					$\frac{2l_\infty}{\pi\xi_0}$	$\frac{2l}{\pi\xi_0}$	$\lambda(t)$
286	770	1590	0.45	2000	0.57	0.5	725
340	730	2370	0.67	4100	1.13	1.0	650

IV. These correction factors would reduce the measured values of λ_0 to values below that of Miller's calculations; to $640\text{--}680 \text{ \AA}$ for sample 286 and $560\text{--}610 \text{ \AA}$ for sample 340. For sample 286, $\xi = 1100 \text{ \AA}$ ($d = 2090 \text{ \AA}$) so the approximation $\xi \gg d$ assumed for the Thompson-Baratoff correction is not obeyed, and the correction factors are only rough estimates.

The experimental error for the measurement of λ_0 for Sn arises from the uncertainty in λ_{Pb} , the error in the thickness measurement of the SiO film, and the uncertainty in relating the measured period to the flux quantum. The uncertainty in the SiO thickness is probably 50 \AA , and this is also the assumed uncertainty in λ_{Pb} . At low temperatures the deviation in the period measurements was $\pm 2\text{--}3\%$ about the mean, which corresponds to an error in λ_0 for Sn of $50\text{--}75 \text{ \AA}$. The sum of the three error contributions gives a total possible uncertainty of $\pm 150 \text{ \AA}$.

Previous experimental results for λ_0 in Sn^{7,11-13,15} hovered in the neighborhood of 510 \AA . These values were obtained from the slope of the $\lambda(t)$ -vs- $Y(t)$ curve, and this result is not λ_0 but $d\lambda/dy$ for $Y > 2$. The BCS theory predicts, and the accurate temperature measurements of λ in Sn by Pippard and Waldram⁷ and by Schawlow and Devlin¹³ confirm, that for small Y ($Y \approx 1.8$) λ deviates from a linear relation with Y . Another measure of the penetration depth is contained in the measurement of the periodicity of the critical current of a single Josephson junction with magnetic field by Fiske.⁶³ His measurements imply a penetration depth of 810 \AA for tin films. Since the thickness and resistivity of the two films that comprised the junction were not reported, it is not possible to compare his result with ours, although both results are in the same neighborhood.

The value of λ_0 could be obtained by plotting $\lambda(t)$ against the BCS temperature dependence instead of Y . For the local BCS temperature dependence this correction would increase the value of 510 \AA by a factor of 1.4. However, Sn is not a local superconductor, so the correction factor is less than 1.4, although it is greater than 1.0. The exact value of this correction is very sensitive to the exact temperature dependence of the energy gap for Sn. With this correction the previous results will be much closer to the BCS predicted value and this work.

TABLE IV. Thompson-Baratoff factors using l_∞ .

Sample	Specular	Diffuse
286	1.13	1.2
340	1.2	1.3

2. Temperature Dependence of λ

The measured temperature dependence of δ for the Sn film of sample 286 is shown in Fig. 9. The experimental values for δ_{Sn} are obtained from the measured field period ΔH by the equation

$$\delta_{\text{Sn}} = \frac{\varphi_0}{\mu w \Delta H} - d - \delta_{\text{Pb}},$$

where δ_{Pb} is calculated from

$$\delta_{\text{Pb}} = \lambda_{\text{Pb}} \left(\frac{w_4}{w} \tanh \frac{d_4}{2\lambda_{\text{Pb}}} + \frac{w_5}{w} \tanh \frac{d_5}{2\lambda_{\text{Pb}}} + \frac{w_{45}}{w} \tanh \frac{d_{45}}{2\lambda_{\text{Pb}}} \right)$$

using $\lambda_0 = 630 \text{ \AA}$ and $\lambda_{\text{Pb}}(t) = \lambda_0 Y(t)$. The values for d_4 , w_4 , etc., are contained in Table I. In the local case δ_{Sn} is related to λ_{Sn} by the relation

$$\delta_{\text{Sn}} = \lambda_{\text{Sn}} \tanh \frac{d}{2\lambda_{\text{Sn}}}.$$

The solid curve in the figure is the calculated value of δ based on Miller's calculations for λ normalized to agree with the experimental value at $Y=0$. The disagreement is manifest. Plotting against Y , however, tends to exaggerate the extent of the disagreement over the temperature range. The experiment and theory start to diverge at $Y=1.25$ which corresponds to $t=0.77$ so that over 75% of the temperature range the sample behavior is as expected. The error bar shown in the curve is the approximate error due to the variation in the period measurement. Any error in λ_{Pb} and the SiO thickness will affect the limiting value of the experimental points at T_c (i. e., at large values of Y); if either λ_{Pb} or d is larger than the value ascribed to it in analyzing the data, the experimental points should be shifted downward by the full amount of the error. If d_1 , the thickness of the Sn film, is larger than the assumed value, the theoretical value at large Y will be shifted upward by one-half the amount of the error. The difference between the theoretical and experimental values at $Y=5.5$ is 250 \AA , and this discrepancy is too large to be accounted for by any reasonable estimate of the experimental error. Sample 340 showed a similar behavior with temperature; the experimental value of δ at $Y=4.3$ is 1200 \AA while the theoretically expected value is 1020 \AA .

Although the local theory has been used to calculate the expected penetration of the field given in Fig. 9, the disagreement between the theory and experiment cannot be removed by a more sophisticated nonlocal analysis of the field distribution within the film. No matter how the field is assumed to penetrate into the film the limiting value of δ at T_c should be one-half the film thickness, or

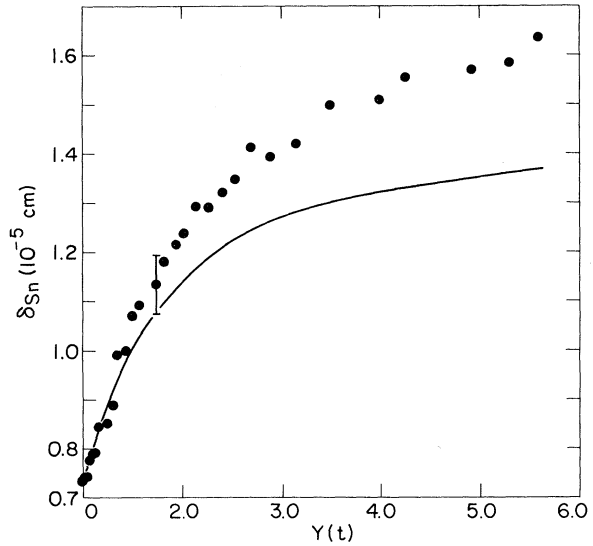


FIG. 9. The measured values of $\delta(t)$ as a function of $Y(t)$ for the Sn film of sample number 286. The solid curve is the theoretically expected behavior based on Miller's calculation of λ and the London expression for δ .

1415 \AA for sample 286, if the film is a homogeneous superconductor with a unique value for λ throughout the film. Simple symmetry considerations require that the current induced by the field increment ΔH be zero at the center of the film if the film is homogeneous and the external field is the same at both surfaces. At T_c the field is essentially uniform throughout the film because the penetration depth is very large. The contribution to the fluxoid from the flux within the film is then $\mu H w d / 2$ since in Eq. (1) the integral contour for the flux is taken along the path where the screening currents vanish, and this path is the center of the film by symmetry.⁶⁴ Thus $\delta(T_c) = d/2$. This limiting value for δ is independent of any particular theory of field penetration into the superconductor.

One possible explanation for this result near T_c is that the film was not homogeneous but instead was under stress which caused a gradient in the order parameter across the thickness of the film. In addition to measuring the penetration depth in his thin-film samples, Lock¹¹ also showed that the enhancement of the critical temperature that is observed in films evaporated on glass substrates is due to strains caused by differential contraction between the substrate and the film at liquid-helium temperatures. He found that when the substrate had a lower coefficient of expansion, e.g., glass substrates, than the metal film, the critical temperature of the film was increased, and when the coefficient was higher the critical temperature was depressed. More recent work has confirmed this effect of strains on T_c of superconducting

films.^{65,66} For the samples used in this experiment the Sn film is evaporated onto a glass substrate and then overlaid with an SiO film, so that at liquid-helium temperatures the Sn is strained at both the top and bottom surfaces. It is unlikely that the evaporated SiO film and glass substrate will strain the Sn in the same manner, and hence, an inhomogeneity is to be expected in the film.

Any inhomogeneity in the film arising from differential strains is likely to produce a gradient in the order parameter. This variation in the order parameter across the thickness of the film would give rise to a position-dependent penetration depth. In this case the model with a constant penetration depth used above to analyze the results is inapplicable. Such a gradient in the order parameter would also affect the superconducting transition.

To try to assess the effect of the overlaid SiO film on the transition temperature of the Sn film, a sample was prepared with a bare Sn film evaporated adjacent to a Sn film that had the usual SiO coverings as described in the beginning of Sec. III. The film overlaid with SiO started to go superconducting 0.02 K above the transition of the uncovered film and both films were completely superconducting at the same temperature. The uncovered film had a transition width of about 0.005 K so the transition of the overlaid film was broadened by 0.015 K. This result supports the view that the SiO overlayer is perturbing the Sn film in some manner which probably destroys the homogeneity of the film.

A simple model was examined in which the strain in the Sn film was assumed to induce a constant gradient in the order parameter across the thickness of the film.²⁵ From the resulting current and field distribution (calculated with the local relations) in the film near T_c , a value for $\delta(T_c)$ can be found. A comparison of this calculated value with the experimentally measured value near T_c determines the magnitude of the gradient in the order parameter, and the broadening of the transition temperature can be calculated from this gradient. The width of the transition temperature calculated in this way agrees remarkably well with the measured width. Thus it seems plausible that strains in the Sn film are responsible for the anomalous effects observed near T_c .

3. Magnetic Field Dependence of λ

It was possible to measure the magnetic field dependence for all field values up to H_c in only one Sn sample. In all Pb samples and in the other Sn sample the junctions "burned out" (the critical current became very large) before a full set of field measurements could be completed. The results

for the one sample are not presented here because a flaw in the design of the sample made it possible that at H_c surface effects were affecting the contour of the circulating currents. The design was corrected, but no subsequent sample held up long enough to make field measurements.

C. Summary of Results and Conclusions

This paper describes the first measurement of the absolute value of the penetration depth in Pb and Sn films apart from a prior tentative result by Meservey¹⁸ for Sn, that is independent of assumptions about the temperature dependence of λ or the frequency dependence of the surface impedance. It was also shown that a double-junction quantum interferometer does not necessarily have period φ_0 in the applied magnetic field in contrast to results obtained in prior investigations.²³

The value for λ_0 in Pb obtained in this experiment is 630 ± 50 Å for a 1500-Å-thick film. Mean-free-path and nonlocal corrections reduce this value to 500–570 Å (depending upon the appropriate boundary condition for scattering at the film surface) which is to be compared with the BCS value of 480 Å for pure bulk Pb. The previously accepted experimental value of 390 Å was obtained by Lock¹¹ from the slope of his $\lambda(t)$ -vs- $Y(t)$ curve. As indicated in Fig. 8 the approximation $\lambda(t) = \lambda_0 Y(t)$ is reasonable for Pb, so his method need not be corrected. His value and the one reported here are not in agreement.

The temperature dependence of λ for Pb was also measured, but these results were limited by the uncertainty in relating the measured field period to the flux quantum. The data allow only the conclusion that the measured temperature dependence is probably in agreement with the recent measurement of Erlback *et al.*⁶¹

For Sn a value for λ_0 of 770 Å was obtained for a film 2830 Å thick with a mean free path $l = 2000$ Å, and a value of 730 Å was obtained for a film 2090 Å thick with $l = 4100$ Å. Approximate nonlocal corrections reduce these values to 640–680 Å ($l = 2000$ Å) and 560–610 Å ($l = 4100$ Å); the corresponding theoretical values calculated by Miller⁶² are 725 Å ($l = 1800$ Å) and 650 Å ($l = 3600$ Å). The agreement between theory and experiment is fairly good. However, the uncertainty in the experimental result may be as large as ± 150 Å, and the nonlocal corrections that were applied do not strictly apply.

Two factors affected the measurement of the temperature dependence of λ in Sn. At low temperatures the error from the uncertainty in the period (caused by the field sensitivity of the junctions as discussed in Sec. II) limited the sensitivity of the measurement to the extent that it was impossible to distinguish between the BCS and Gor-

ter-Casimir behavior. Near T_c the results were affected in some manner not understood, but the effect was tentatively ascribed to strains. These

two limitations made it impossible to obtain data for λ as a function of temperature that could be compared with theory or prior experiments.

*Work supported by NASA and The Air Force Office of Scientific Research and the National Science Foundation.

†Present address: Urban Institute, 2100 M Street N. W., Washington, D. C. 20037.

‡Now supported by the National Science Foundation.

¹F. London and H. London, Proc. Roy. Soc. (London) A149, 71 (1935).

²D. Shoenberg, Proc. Roy. Soc. (London) A175, 49 (1940).

³D. Shoenberg, *Superconductivity* (Cambridge U. P., Cambridge, England, 1952).

⁴F. London, *Superfluids* (Wiley, New York, 1950), Vol. 1.

⁵B. Serin, in *Handbuch der Physik*, edited by S. Flügge (Springer-Verlag, Berlin, 1956), Vol. 15, p. 210.

⁶R. Jaggi and R. Sommerhalder, Helv. Phys. Acta 33, 1 (1960).

⁷J. R. Waldram, Advan. Phys. 13, 1 (1964).

⁸R. Meservey and B. B. Schwartz, in *Superconductivity*, edited by R. D. Parks (Marcel Dekker, New York, 1969), Vol. 1, p. 117.

⁹C. S. Whitehead, Proc. Roy. Soc. (London) A238, 175 (1957).

¹⁰M. Désirant and D. Shoenberg, Proc. Roy. Soc. (London) 60, 413 (1948).

¹¹J. M. Lock, Proc. Roy. Soc. (London) A208, 391 (1951).

¹²E. Laurmann and D. Shoenberg, Proc. Roy. Soc. (London) A198, 560 (1949).

¹³A. L. Schawlow and G. E. Devlin, Phys. Rev. 113, 120 (1959).

¹⁴H. London, Proc. Roy. Soc. (London) A176, 522 (1940).

¹⁵A. B. Pippard, Proc. Roy. Soc. (London) A191, 370 (1947); A191, 385 (1947); A191, 399 (1947); A203, 98 (1950); A203, 195 (1950).

¹⁶A. B. Pippard, Proc. Roy. Soc. (London) A203, 210 (1950).

¹⁷M. P. Garfunkel, Phys. Rev. 173, 516 (1968).

¹⁸R. Meservey, in *Proceedings of the Ninth International Conference on Low Temperature Physics*, edited by J. G. Daunt, D. O. Edwards, F. J. Milford, and M. Yaqub (Plenum, New York, 1965), p. 455.

¹⁹L. Onsager, Phys. Rev. Letters 7, 50 (1961).

²⁰W. Meissner and R. Ochsenfeld, Naturwiss. 21, 787 (1933).

²¹B. D. Josephson, Phys. Letters 1, 251 (1962); Advan. Phys. 14, 419 (1962).

²²J. M. Rowell, Phys. Rev. Letters 11, 200 (1963).

²³R. C. Jaklevic, J. Lambe, J. E. Mercereau, and A. H. Silver, Phys. Rev. 140, A1628 (1965). See also the review by J. E. Mercereau, in Ref. 8, Vol. 1, p. 393.

²⁴R. de Bruyn Ouboter and A. Th. A. M. de Waele, in *Progress in Low Temperature Physics*, edited by C. J. Gorter (North-Holland, Amsterdam, 1970), Vol. 6.

²⁵G. E. Peabody, Ph.D. thesis (Harvard University, 1969) (unpublished).

²⁶T. A. Fulton, Solid State Commun. 8, 1353 (1970).

²⁷A. H. Silver and J. E. Zimmerman, Phys. Rev. 157,

317 (1967); A. Th. A. M. de Waele, W. H. Kraan, and R. de Bruyn Ouboter, Physica 40, 302 (1968).

²⁸R. Meservey, J. Appl. Phys. 39, 2598 (1968); J. Clarke, Phil. Mag. 13, 115 (1966).

²⁹J. E. Zimmerman and A. H. Silver, Phys. Rev. 141, 367 (1966).

³⁰P. W. Anderson and A. H. Dayem, Phys. Rev. Letters 13, 195 (1964).

³¹J. Clarke, in *Proceedings of the Tenth International Conference on Low-Temperature Physics, Moscow, 1966*, edited by M. P. Malkov (Proizvodstvenno-Izdatel'skii Kombinat, VINITI, Moscow, 1967).

³²J. E. Zimmerman and A. H. Silver, Phys. Letters 10, 47 (1964).

³³P. W. Anderson, in *Lectures on the Many-Body Problem, Ravello, 1963*, edited by E. R. Caivano (Academic, New York, 1964), Vol. 2, p. 115; *Progress in Low Temperature Physics*, edited by C. J. Gorter (North-Holland, Amsterdam, 1967), Vol. 5, p. 1.

³⁴B. B. Schwartz and A. Baratoff, Bull. Am. Phys. Soc. 12, 76 (1967).

³⁵J. E. Zimmerman and A. H. Silver, Solid State Commun. 4, 133 (1966); A. H. Silver and J. E. Zimmerman, Phys. Rev. 157, 317 (1967).

³⁶A. H. Dayem and J. J. Wiegand, Phys. Rev. 155, 419 (1967).

³⁷I. Giaever, Phys. Rev. Letters 5, 147 (1960); 5, 464 (1960); I. Giaever and K. Megerle, Phys. Rev. 122, 1101 (1961).

³⁸A. I. Larkin and Yu. N. Ovchinnikov, Zh. Eksperim. i Teor. Fiz. 51, 1535 (1966) [Sov. Phys. JETP 24, 1035 (1967)].

³⁹M. Peter, Phys. Rev. 109, 1857 (1958); F. M. Odeh, J. Math. Phys. 5, 1168 (1964).

⁴⁰J. R. Schrieffer, Phys. Rev. 106, 47 (1957).

⁴¹A. M. Toxen, Phys. Rev. 123, 442 (1961); 127, 382 (1962).

⁴²A. M. Toxen and M. J. Burns, Phys. Rev. 130, 1808 (1963).

⁴³M. Tinkham, Phys. Rev. 110, 26 (1958).

⁴⁴W. Ittner, III, Phys. Rev. 119, 1591 (1960).

⁴⁵R. S. Thompson and A. Baratoff, Phys. Rev. 167, 361 (1968).

⁴⁶Allen Jones Electronics Corp., 17171 S. Western Ave., Gardena, Calif.

⁴⁷Vacuum Atmospheres Corp., 4652 W. Rosecrans Ave., Hawthorne, Calif. 90250.

⁴⁸W. Schroen, J. Appl. Phys. 39, 2671 (1968).

⁴⁹C. Blake and C. E. Chase, Rev. Sci. Instr. 34, 984 (1963).

⁵⁰S. Cunsolo, M. Santini, and M. Vincentini-Missoni, Cryogenics 5, 168 (1965).

⁵¹D. B. Montgomery, *Solenoid Magnet Design* (Wiley, New York, 1969).

⁵²D. D. Coon and M. D. Fiske, Phys. Rev. 138, A744 (1965).

⁵³Hilger and Watts, Ltd., London, England; H. E. Bennett and J. M. Bennett, in *Physics of Thin Films*, edited by G. Hass and R. E. Thun (Academic, New York, 1964), Vol. 2.

- ⁵⁵J. Bardeen and R. Schrieffer, in *Progress in Low Temperature Physics*, edited by C. J. Gorter (North-Holland, Amsterdam, 1967), Vol. 3, p. 170.
- ⁵⁶J. C. Swihart and W. Shaw (unpublished).
- ⁵⁷A. B. Pippard, Proc. Roy. Soc. (London) **A216**, 547 (1963).
- ⁵⁸R. G. Chambers, Proc. Roy. Soc. (London) **A215**, 481 (1952).
- ⁵⁹J. Millstein and M. Tinkham, Phys. Rev. **158**, 3. (1967).
- ⁶⁰V. L. Newhouse, *Applied Superconductivity* (Wiley, New York, 1964), p. 108.
- ⁶¹E. Erlbach, R. L. Garwin, and M. P. Sarachik, IBM J. Res. Develop. **4**, 107 (1960); M. P. Sarachik, R. L. Garwin, and E. Erlbach, Phys. Rev. Letters **4**, 52 (1960).
- ⁶²P. B. Miller, Phys. Rev. **113**, 1209 (1959).
- ⁶³M. D. Fiske, Rev. Mod. Phys. **36**, 221 (1964).
- ⁶⁴The claim here is not that the total field within the film is symmetrically distributed, but that the field increment added to change the number of fluxoids from n to $(n+1)$ is. The total current, including the bias current, is undoubtedly not zero at the center of the film. But this experiment measures the change in current as each fluxoid is added to the loop and this induced current is zero at the center of the film.
- ⁶⁵A. M. Toxen, Phys. Rev. **123**, 442 (1963).
- ⁶⁶B. W. Friday and J. L. Mundy, J. Appl. Phys. **40**, 2162 (1969).

Thermal Conductivity of Superconducting Lead-Indium Alloys^{*†}

A. K. Gupta and S. Wolf

Department of Physics, Case Western Reserve University, Cleveland, Ohio 44106

(Received 7 February 1972)

The thermal conductivity in the mixed state K_m of a series of lead-indium alloys containing from 3 to 21 at. % In was measured as a function of temperature and magnetic field. The temperature dependence of the thermal conductivities in the superconducting and normal states K_s and K_n , respectively, was also measured in the range from 1.35 to 7.5 K. In the mixed state, the main emphasis was on the region near the upper critical field H_{c2} where Caroli and Cyrot found theoretically that the electronic thermal conductivity of dirty type-II superconductors varies linearly with applied magnetic field. In order to compare with their theory it was necessary to separate the electronic and lattice thermal conductivities, and to analyze the lattice contribution in terms of the scattering by boundaries, point defects, and conduction electrons. The field dependence of the lattice thermal conductivity was then theoretically calculated and subtracted from the experimentally measured field dependence of the total thermal conductivity. The experimental results are in good agreement in the dirty limit but large deviations are observed as the indium concentration is reduced. The phonon mean free path due to scattering by point defects was found to be in reasonably good agreement with the Klemens theory. The upper critical fields H_{c2} obtained from K -vs- H curves were compared with the theory of Helfand and Werthamer. From the critical fields, the product of the electronic mean free path and the residual electrical resistivity was found to be $0.66 \times 10^{-11} \Omega \text{ cm}^2$. The coherence length in the pure limit ξ_0 was also computed from the data and a value of 1060 Å was found.

I. INTRODUCTION

The thermal conductivity of type-II superconducting alloys as a function of magnetic field, under certain circumstances, is observed to go through a minimum. Minima in the variation of thermal conductivity with magnetic field can also occur when an intermediate-state structure exists, and since early measurements¹⁻⁴ focused on the intermediate state the distinctive behavior of type-II superconductors was not at first recognized. Sladek⁵ was the first to observe a minimum for In-Tl alloys even in the absence of the intermediate state. This work went unnoticed until Dubeck *et al.*⁶ observed similar behavior for In-Bi alloys. They explained this behavior by considering the variation of the

spatially averaged energy gap with field and the dependence of the thermal conductivity on the energy gap as calculated by Bardeen, Rickayzen, and Tewordt (BRT).⁷ They showed that the phonon conductivity should rapidly decrease as the magnetic field is increased beyond the lower critical field H_{c1} . For higher values of the field the phonon conductivity should decrease slowly and should reach the normal-state value at $H = H_{c2}$. At the same time the electronic thermal conductivity increases towards its value in the normal state as the field increases from H_{c1} to H_{c2} . The combination of the two effects yields the observed behavior. The depth of the minimum depends on the ratio of the thermal conductivity in the superconducting state to the normal state. When the conductivity